

CONTINUOUS MATHEMATICAL MODELS OF AIRLIFT BIOREACTORS: FAMILIES, AFFINITY, DIVERSITY AND MODELLING FOR SINGLE-SUBSTRATE KINETICS

Robert Grzywacz*

Cracow University of Technology, Institute of Chemical and Process Engineering,
ul. Warszawska 24, 31-155 Cracow, Poland

This paper presents a method of describing an airlift bioreactor, in which biodegradation of a carbonaceous substrate described by single-substrate kinetics takes place. Eight mathematical models based on the assumption of liquid plug flow and axial dispersion flow through the riser and the downcomer in the reactor were proposed. Additionally, the impact of degassing zone with assumed complete mixing on the obtained results was analyzed. Calculations were performed for two representative hydrodynamic regimes of reactor operation, i.e. with the presence of gas bubbles only within the riser and for complete gas circulation. The conclusions related to the apparatus design and process performance under sufficient aeration of the reaction mixture were drawn on the basis of the obtained results.

Keywords: airlift bioreactor, single-substrate kinetics, mathematical modelling, simulation, multiphase reactors

1. INTRODUCTION

Airlift reactors have been widely applied in chemical and biochemical industry to conduct two- or three-phase processes characterised by slow reactions in the liquid phase or biofilm (Camarasa et al., 2001).

The analysis of state-of-the-art of research on airlift reactors shows that authors are particularly interested in hydrodynamics and mass transfer in the apparatus. Typical results on this subject matter can be found in papers (Gavrilescu et al., 1998; Korpajarvi et al., 1999; Vial et al., 2001).

Knowledge about adequate mathematical models is required for the proper design of each type of reactor. Airlift bioreactors are characterised by a significant hydrodynamic complexity. It results from the existence of some hydrodynamic zones related to a characteristic geometrical structure of the reactor. Additionally, two main operation states of the reactor can be observed in regard to the process. The first one is observed when gas bubbles are present only in the raiser, and the other one when gas bubbles are present in each hydrodynamic zone of the reactor. These both states are further referred to as hydrodynamic regimes of the reactor operation. The assumed kinetic model of the process has an extra impact on the complex description of the airlift bioreactor operation.

Due to such complexity of the model, it is possible to form a family of its mathematical models. The set of all such models with the same number of limiting substrates will be known as the family of mathematical models for airlift bioreactors. In other words, the number of limiting substrates is the

*Corresponding author, e-mail: robekk@gmail.com

family invariant. Thus, we can refer to families of single-substrate, two-substrate, etc. models. According to this family definition, the number of equations for a given model depends on its attachment to a given family, and additionally on the number of distinguished hydrodynamic zones in a bioreactor.

Examples of published mathematical models of airlift reactor can be found in many papers (Báleš et al., 1999; Boyadjiev, 2006; Kanai et al., 1996; 2000; Marchuk et al., 1980; Sikula and Markoš, 2008; Znad et al., 2004). The majority of published mathematical models are based on tank-in-series approximation to describe the structure of media flow or to solve the axial dispersion model by discretisation method. Bearing in mind the above, this paper is only focused on a group of models expressed by differential equations and their direct solutions, without performing preliminary discretisation. These models are called continuous models.

This paper presents the modelling methods of airlift bioreactor, in which biodegradation of carbonaceous substrate is conducted by an adequately selected bacteria strain. Single-substrate kinetics was adopted to describe the process. Therefore, all the models presented in this paper belong to the family of single-substrate models.

The reactor operation in both above-mentioned hydrodynamic regimes was analysed. Two sets of hydrodynamic zones in the bioreactor were distinguished. The first one, consisting of the riser and downcomer, and the other one which additionally includes the degassing zone.

The plug flow or axial dispersion flow models, both expressed by appropriate differential equations, were adopted as the structure of media flow through the riser and downcomer. The model of complete mixing which included the degassing zone was adopted for the study.

2. THEORY OF AIRLIFT BIOREACTORS OPERATION

The airlift bioreactor can be classified as a bubble column bioreactor with recirculation, owing to the nature of media flow inside it. There are two basic apparatus projects of the work of such reactors. One covers the apparatus with an external loop and the other one with an internal loop. A scheme of conceptual media flow structure in the airlift reactor is presented in Figure 1. In both constructional cases, the reactor consists of four hydrodynamic zones: zone *I* (riser), in which the gas-liquid mixture rises towards the upper part of the apparatus, and zone *II* (downcomer), in which the partially or completely degassed mixture falls towards the reactor bottom, zone *III* known as the degassing zone, in which gas-liquid mixture is partially or completely degassed and the bottom zone *IV*.

Depending on whether the gas-liquid mixture undergoes partial or complete degassing in zone *III*, we can distinguish three hydrodynamic regimes of reactor operation. Their presence is closely related to the gas flow rate and design of the bioreactor.

Regime *A* – liquid circulation between the riser and the downcomer is not large for a low gas volumetric flow rate. Liquid velocity in the annular downcomer zone is then lower than gas bubbles slip velocity. It means that the gas phase is present only in the riser. An increase in gas velocity causes an increase in the gas hold-up in the riser at zero value in the downcomer.

Regime *B* – liquid circulation in the downcomer increases along with the velocity increase in the fed gas, and at some moment it reaches gas bubbles slip velocity. This is the border between 1st and 2nd regime of the reactor operation. Further increase in gas velocity will result in the downcomer gradual filling with gas bubbles, but without any effect on velocity change of the circulating liquid as the difference in the riser and the downcomer gas hold-up is constant. The downcomer gas flow rate still equals zero.

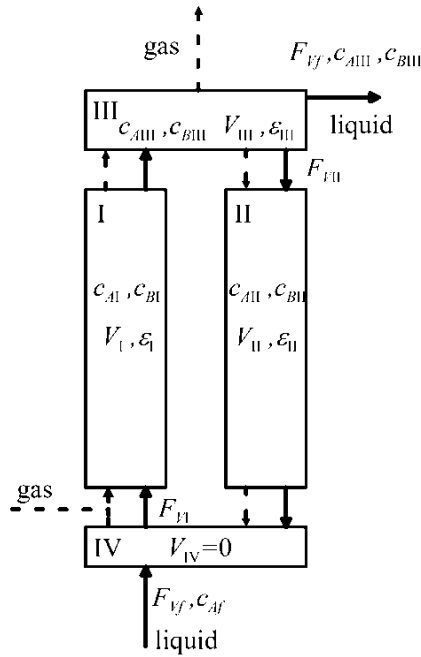


Fig. 1. Schematic diagram of hydrodynamic zone and media flow structure in airlift bioreactor

Regime *C* – by increasing the gas flow rate, it will reach the value at which the downcomer liquid flow will exceed gas bubbles slip velocity. Then, the gas phase starts to circulate between the riser and the downcomer. During gas flow rate increase in this operation regime, also gas hold-up in both zones as well as liquid circulation velocity increase. Downcomer gas velocity is higher than zero and has the same direction as the liquid.

Beside the impact of gas flow rate on hydrodynamic regime change, some impact of liquid flow rate, reactors geometry and designing solutions is also observed. The hydrodynamic regimes described above are presented in Figure 2.

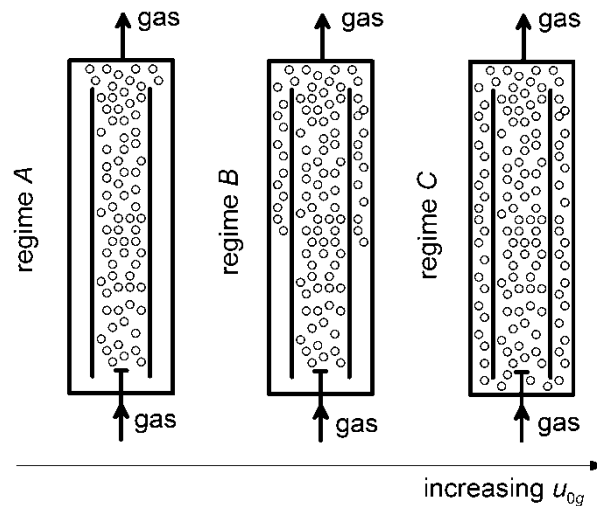


Fig. 2. Hydrodynamic regimes of airlift reactor operation and idea of their formation

Considering the above aspects of airlift reactors operation, it is necessary to define the hydrodynamic region for the modelled reactor operation prior to mathematical model formulation. The reactor

operation in two regimes, i.e. regime *A* and *C* was analysed in this paper. Regime *A* is representative for bioreactors with a liquid external loop, and regime *C* for reactors with a liquid internal loop. All the calculations included in the work were determined for a reactor with internal circulation of the liquid.

Apart from determining the hydrodynamic regime for the reactor operation, it is also required to adopt media flow structure in distinguished hydrodynamic zones. In this paper, it was assumed that for zones *I* and *II* the liquid phase is described by plug flow or axial dispersion flow, whereas for other zones it was assumed that zone *IV* is negligibly small and it will be substituted by equations for mixing node in the model. On the other hand, two different cases were analysed for zone *III*. In the first case, similarly as for zone *IV*, its zero volume was assumed, and in the other case, the zone volume is not disregarded, and thus complete mixing is assumed to occur inside it. For these assumed media flow streams (Figure 1), carbonaceous substrate concentration at zone *I* outlet decides on the biodegradation yield providing that there is no degassing zone. In other cases, concentration at the degassing zone outlet has a decisive importance. While a bioreactor is being designed, parameters should be selected in order to minimise this concentration value.

3. AIRLIFT REACTOR HYDRODYNAMICS

The previously mentioned phenomena should be taken into consideration and quantitatively described in the model equations in order to include the assumed hydrodynamic regimes, namely regime *A* or *C*, in which the analysed reactor operates.

Regime A

In compliance with the previously presented hydrodynamic characteristics, in this regime $\varepsilon_{gII} = 0$ and $u_{III} < v$, where v is gas bubbles slip velocity. Gas and liquid balances in the bioreactor can be expressed by Equations (1a) and (1b)

$$S_I \varepsilon_{gI} (u_{II} + v) = S_I u_{0g} \quad (1a)$$

$$S_I (1 - \varepsilon_{gI}) u_{II} = S_I u_{0l} + S_{II} u_{III} \quad (1b)$$

where $u_{0g} = \frac{F_V^g}{S_I}$ and $u_{0l} = \frac{F_V^l}{S_I}$.

Among the equations constituting the hydrodynamic model of airlift reactors, there is an expression which equates buoyancy force formed by the difference in medium density in zones *I* and *II* with the resultant force of hydrodynamic resistances related to liquid motion. Such a formulation was used in, inter alia, elsewhere (Heijnen et al., 1997). The analogical reasoning was applied below. So, Equation (1c) is for regime *A*

$$gH_I \varepsilon_{gI} = 0.5 \left[(k_{fI} + k_{fIII}) u_{II}^2 + (k_{fII} + k_{fIV}) u_{III}^2 \right] \quad (1c)$$

where: H_I is height of liquid phase in the reactor, k_f is flow resistance coefficient in adequate zones of the reactor, ε_g is gas hold-up in an adequate zone, and u_l is liquid flow velocity.

Regime C

At sufficiently high gas flow rates, $u_{III} > v$, so $u_{gII} = u_{III} - v$. Then, we obtain

$$S_I \varepsilon_{gI} (u_{II} + v) = S_I u_{0g} + S_{II} \varepsilon_{gII} (u_{III} - v) \quad (2a)$$

$$S_I (1 - \varepsilon_{gI}) u_{II} = S_I u_{0l} + S_{II} (1 - \varepsilon_{gII}) u_{III} \quad (2b)$$

$$gH_I (\varepsilon_{gI} - \varepsilon_{gII}) = 0.5 \left[(k_{fI} + k_{fIII}) u_{II}^2 + (k_{fII} + k_{fIV}) u_{III}^2 \right] \quad (2c)$$

If liquid flow velocity in zones *I* and *II* is combined by continuity equation, then the systems of three Equations (1) and (2) can be reduced to the systems of two equations with two unknowns: ε_{gI} and u_{II} . They are presented below.

Regime A

$$\varepsilon_{gI}(u_{II} + v) - u_{0g} = 0 \quad (3a)$$

$$gH_I \varepsilon_{gI} - 0.5[(k_{fI} + k_{fIII})u_{II}^2 + (k_{fII} + k_{fIV})u_{III}^2] = 0 \quad (3b)$$

where $u_{III} = \frac{S_I}{S_{II}} [(1 - \varepsilon_{gI})u_{II} - u_{0I}]$.

Regime C

$$\varepsilon_{gI}(u_{II} + v) - \frac{S_{II}}{S_I} \varepsilon_{gII}(u_{III} - v) - u_{0g} = 0 \quad (4a)$$

$$gH_I (\varepsilon_{gI} - \varepsilon_{gII}) - 0.5[(k_{fI} + k_{fIII})u_{II}^2 + (k_{fII} + k_{fIV})u_{III}^2] = 0 \quad (4b)$$

where $u_{III} = \frac{S_I}{S_{II}} \left(\frac{1 - \varepsilon_{gI}}{1 - \varepsilon_{gII}} u_{II} - \frac{u_{0I}}{1 - \varepsilon_{gII}} \right)$.

The expression defining gas bubbles slip velocity v can be found elsewhere (Garcia-Calvo et al., 1991),

namely $v = 1.53 \left(\frac{g\sigma(\rho_l - \rho_g)}{\rho_l^2} \right)^{0.25}$.

By solving the systems of Equations (3) and (4) for hydrodynamic regimes *A* and *C*, the values of gas hold-up, liquid flow velocity and gas flow velocity for zones *I* and *II* are obtained. These equations can also be used to determine borders between particular hydrodynamic regimes. The experimental verification of the proposed model is presented in the earlier papers (Grzywacz, 2008 and 2009).

It should be stated that solutions of hydrodynamic equations allow to obtain mean values of gas hold-up. If the reactor operates in hydrodynamic regimes *A* and *C*, it is correct to adopt mean values of gas hold-up for further project calculations. However, such an assumption is wrong for the reactor operation in the hydrodynamic regime *B*. The formation of border between gassing and degassing zone in the downcomer is observed for this regime. The location of this border depends on gas flow rate and, along with its increase, it is moved towards the column bottom. No suggestions have so far been put forward for solving this problem other than by models based on Computational Fluid Dynamics (CFD).

4. KINETICS OF PHENOL BIODEGRADATION

Aerobic biodegradation of phenol in the bioreactor was assumed as the process example. If the reaction medium is sufficiently aerate, then the process occurs in the kinetic regime (Grzywacz and Lubaś, 2006), and single-substrate kinetics are used for its description. Biomass growth is limited only by the carbonaceous substrate. The uptake rate of carbonaceous substrate r_A and the growth rate of biomass r_B are expressed by these formulas:

$$r_A(c_A, c_B) = \frac{1}{w_{BA}} f(c_A) \cdot c_B \quad (5)$$

$$r_B(c_A, c_B) = f(c_A) \cdot c_B \quad (6)$$

where w_{AB} – biomass yield coefficient, and $f(c_A)$ – specific growth rate of microorganisms.

Also Haldane equation (Pawlowsky and Howell, 1973) was used in this paper:

$$f(c_A) = \frac{k \cdot c_A}{K_A + c_A + \frac{c_A^2}{K_{in}}} \quad (7)$$

The following values of *kinetic* parameters were assumed for further quantitative analysis (Pawlowsky and Howell, 1973): $k = 0.26$ [1/h], $K_A = 0.0254$ [kg/m³], $K_{in} = 0.173$ [kg/m³] i $w_{BA} = 0.616$ [kgB/kgA].

5. MATHEMATICAL MODEL OF AIRLIFT BIOREACTOR

While developing a bioreactor mathematical model, an adequate number of equations required for its description should be formulated. The number of these equations depends on the process kinetics and the number of zones undergoing balancing.

Biodegradation is conducted in the airlift bioreactor, which geometry indicates the existence of four already described hydrodynamic zones. For modelling purposes, plug flow or axial dispersion flow of media was assumed in zones *I* and *II*. The assumed axial dispersion model allows to test a wide range of Peclet number variability. For high Peclet numbers, after the application of the plug flow model, it is possible to significantly simplify numerical calculations.

Each model was prepared for two hydrodynamic regimes of reactor operation, i.e. for regime *A* and *C*. Both cases included the presence or absence of degassing zone *III*.

The following symbols were used in this paper to order and distinguish the proposed models: PFM –plug flow model in zones *I* and *II*, ADM –axial dispersion model for media flow in zones *I* and *II*. The symbol of hydrodynamic regime for reactor operation follows the dash, i.e. *A* – for hydrodynamic regime *A* and *C* – for hydrodynamic regime *C*. Then, the next dash introduces the presence (D) or lack of the degassing zone. For example, ADM-C-D stands for an axial dispersion model in zones *I* and *II* for the reactor operating in hydrodynamic regime *C* and defines the presence of the degassing zone.

Since a single-substrate family is examined and the aerobic process is analysed, a sufficient aeration of the liquid phase seems to be assumed. If this is the case there is no need to formulate oxygen balances. This means that gas phase in the system influences only its hydrodynamics.

The following algorithm was taken for further mathematical models formulation. The plug flow model in zones *I* and *II* as well as the axial dispersion model in zones *I* and *II* were discussed independently. At first, this analysis was performed for hydrodynamic regime *A*, and then for regime *C*. The model without distinguished zone *III* was discussed first, and then the model that included the zone. This allows for gradual modification of all the formulated equations and stepwise addition of next balance equations in compliance with assumptions related to bioreactor design and process performance conditions. The model symbol is given in brackets.

5.1. Model No. 1 – plug flow in zones *I* and *II*, lack of zone *III*, hydrodynamic regime *A* (PFM-A)

The equations of carbonaceous substrate and microorganisms mass balances in the liquid phase for the steady state are as follows:

$$u_{II} \frac{dc_{AI}}{dh} = -r_A(c_{AI}, c_{BI}) \quad (8a)$$

$$u_{II} \frac{dc_{BI}}{dh} = r_B(c_{AI}, c_{BI}) \quad (8b)$$

$$u_{III} \frac{dc_{AII}}{dh} = -r_A(c_{AII}, c_{BII}) \quad (8c)$$

$$u_{III} \frac{dc_{BII}}{dh} = r_B(c_{AII}, c_{BII}) \quad (8d)$$

Equations (8) should be completed with expressions including the presence of circulation liquid and fresh raw material mixing node, i.e.:

$$F_{Vf} + F_{VII} = F_{VI} \quad (9a)$$

$$F_{Vf}c_{Af} + F_{VII}c_{AII}(H_{II}) = F_{VI}c_{A0} \quad (9b)$$

$$F_{VII}c_{BII}(H_{II}) = F_{VI}c_{B0} \quad (9c)$$

By introducing Equation (9a) to (9b) and (9c) and by defining recirculation ratio as

$$\xi = \frac{F_{VII}}{F_{VI}} \quad (10)$$

for the mixing node we obtain:

$$(1 - \xi)c_{Af} + \xi \cdot c_{AII} = c_{A0} \quad (11a)$$

$$\xi \cdot c_{BII} = c_{B0} \quad (11b)$$

As the riser and downcomer volumes can be different, the coefficient determining zone *I* volume ratio to the sum of reactor zone *I* and *II* volumes was defined:

$$\zeta_1 = \frac{V_I}{V} = \frac{V_I}{V_I + V_{II}} \quad (12)$$

According to Equation (9), zone *I* and *II* volumes are $V_I = \zeta_1 \cdot V$ and $V_{II} = (1 - \zeta_1)V$

The liquid phase residence time in zone *I* can be defined as:

$$\tau_I = \frac{V_I(1 - \varepsilon_1)}{F_{VI}} \quad (13)$$

and the liquid phase residence time in zone *II* can be defined as:

$$\tau_{II} = \frac{V_{II}}{F_{VII}} \quad (14)$$

By introducing previously defined recycle ratio ξ and volume distribution coefficient ζ_I to Equations (13) and (14), we obtain the final expression for residence times in zones *I* and *II*:

$$\tau_I = \zeta_1 \cdot \tau \cdot (1 - \varepsilon_1) \cdot (1 - \xi) \quad (15)$$

$$\tau_{II} = (1 - \zeta_1) \cdot \tau \cdot \frac{(1 - \xi)}{\xi} \quad (16)$$

$$\text{where } \tau = \frac{V_I + V_{II}}{F_{Vf}}$$

Now, the relationship for determining recirculation ratio, ξ , is to be defined. According to Formula (10), and after determining liquid velocity in zones *I* and *II* from the hydrodynamic model it can be described as:

$$\xi = \frac{u_{III}(1 - \varepsilon_{II})(1 - \zeta_I)}{u_{II}(1 - \varepsilon_I)\zeta_I} \quad (17)$$

Dimensionless state variables will be introduced for further analysis. They are: degree of conversion of the carbonaceous substrate, α , and dimensionless concentration of biomass, β , defined respectively as:

$$\alpha_i = \frac{c_{Af} - c_{Ai}}{c_{Af}} \quad (18a)$$

$$\beta_i = \frac{c_{Bi}}{c_{Af}} \quad (18b)$$

By introducing the above-defined dimensionless state variables α and β , model parameters and reactor dimensionless length $z = h/H$ to Equations (8), a system of 4 differential equations with boundary conditions defined for $z = 0$ and for $z = 1$ is obtained

$$\frac{d\alpha_I}{dz} = \tau_I r_A(\alpha_I, \beta_I) \quad (19a)$$

$$\frac{d\beta_I}{dz} = \tau_I r_B(\alpha_I, \beta_I) \quad (19b)$$

$$\frac{d\alpha_{II}}{dz} = \tau_{II} r_A(\alpha_{II}, \beta_{II}) \quad (19c)$$

$$\frac{d\beta_{II}}{dz} = \tau_{II} r_B(\alpha_{II}, \beta_{II}) \quad (19d)$$

$$\alpha_I(0) = \alpha_0 \quad (20a)$$

$$\beta_I(0) = \beta_0 \quad (20b)$$

$$\alpha_{II}(0) = \alpha_I(1) \quad (20c)$$

$$\beta_{II}(0) = \beta_I(1) \quad (20d)$$

along with algebraic equations characterising the mixing node:

$$\alpha_0 - \xi\alpha_{II}(1) = 0 \quad (21a)$$

$$\xi\beta_{II}(1) - \beta_0 = 0 \quad (21b)$$

5.2. Model No. 2 – plug flow in zones *I* and *II*, complete mixing in zone *III*, hydrodynamic regime *A* (PFM-A-D)

Mass balance Equations (19) should be completed with carbonaceous substrate and biomass balances equations in zone *III* on the assumption of complete mixing, in order to include the presence of mentioned zone *III*. Hence, we obtain:

$$\frac{1}{\tau_{III}}(\alpha_I(1) - \alpha_{III}) + r_A(\alpha_{III}, \beta_{III}) = 0 \quad (22a)$$

$$\frac{1}{\tau_{III}}(\beta_I(1) - \beta_{III}) + r_B(\alpha_{III}, \beta_{III}) = 0 \quad (22b)$$

Additionally, initial conditions for zone II should be modified:

$$\alpha_{II}(0) = \alpha_{III} \quad (23a)$$

$$\beta_{II}(0) = \beta_{III} \quad (23b)$$

Beside balance equations, also some parameters of the considered models will be redefined and modified. Thus, volume distribution coefficients were now defined in the following way:

$$\zeta_i = \frac{V_i}{V} = \frac{V_i}{\sum_i V_i} \quad \text{for } i = I, II, III \quad (24)$$

Liquid mean residence times in individual zones are then calculated as follows:

$$\tau_I = \zeta_I \cdot \tau \cdot (1 - \varepsilon_I) \cdot (1 - \zeta) \quad (25a)$$

$$\tau_{II} = \zeta_{II} \cdot \tau \cdot \frac{(1 - \zeta)}{\zeta} \quad (25b)$$

$$\tau_{III} = \zeta_{III} \cdot \tau \cdot (1 - \varepsilon_{III}) \cdot (1 - \zeta) \quad (25c)$$

5.3. Model No. 3 – plug flow in zones I and II, lack of zone III, hydrodynamic regime C (PFM-C)

The next modification of the plug flow model is based on formulating equations which describe the reactor operation in hydrodynamic regime C. It turned out that the dimensionless form of the model is identical with Equations (19) and conditions (20). The only change relates to the expression of liquid residence time in zone II. Therefore, Equation (14) was modified to the form below:

$$\tau_{II} = \frac{V_{II}(1 - \varepsilon_{II})}{F_{VII}} \quad (26)$$

and

$$\tau_{II} = (1 - \zeta_I) \cdot \tau \cdot (1 - \varepsilon_{II}) \frac{(1 - \zeta)}{\zeta} \quad (27)$$

The other equations and expressions are formulated as in model No. 1.

5.4. Model No. 4 – plug flow in zones I and II, complete mixing in zone III, hydrodynamic regime C (PFM-C-D)

Model No. 4 indicated as PFM-C-D contains modifications introduced during the formulation of models No. 2 and No. 3. It means that the final form of balance equations is identical with equations for model No. 2. The difference is related to liquid phase residence time in zone II, namely:

$$\tau_{II} = \zeta_{II} \cdot \tau \cdot (1 - \varepsilon_{II}) \frac{(1 - \zeta)}{\zeta} \quad (28)$$

As can be observed, mathematical models formulated for plug flow in zones *I* and *II* contain a kind of balance equations core completed with an additional equation if zone *III* is present. So, it can be said that there are similarities between these models for the assumed media flow. This similarity was taken into account when accepting the discussion order of individual models.

Then, the way of forming models for dispersion flow in zone *I* and *II* will be presented. As previously, models formulation will begin from the simplest case and then, further modifications and additional balance equations will be introduced as the model complexity level is increasing.

5.5. Model No. 5 – dispersion flow in zones *I* and *II*, lack of zone *III*, hydrodynamic regime *A* (ADM-A)

The mass balance equations of carbonaceous substrate *A* and microorganisms *B* for the assumed flow have the following form:

$$D_{mI} \frac{d^2 c_{AI}}{dh^2} - u_{II} \frac{dc_{AI}}{dh} - r_A(c_{AI}, c_{BI}) = 0 \quad (29a)$$

$$D_{mI} \frac{d^2 c_{BI}}{dh^2} - u_{II} \frac{dc_{BI}}{dh} + r_B(c_{AI}, c_{BI}) = 0 \quad (29b)$$

$$D_{mII} \frac{d^2 c_{AII}}{dh^2} - u_{III} \frac{dc_{AII}}{dh} - r_A(c_{AII}, c_{BII}) = 0 \quad (29c)$$

$$D_{mII} \frac{d^2 c_{BII}}{dh^2} - u_{III} \frac{dc_{BII}}{dh} + r_B(c_{AII}, c_{BII}) = 0 \quad (29d)$$

The mixing node equations are identical with Equations (11).

After introducing previously defined dimensionless values to Equations (29), the following forms of model equations are obtained:

$$\frac{1}{Pe_I} \frac{d^2 \alpha_I}{dz^2} - \frac{d\alpha_I}{dz} + \tau_I r_A(\alpha_I, \beta_I) = 0 \quad (30a)$$

$$\frac{1}{Pe_I} \frac{d^2 \beta_I}{dz^2} - \frac{d\beta_I}{dz} + \tau_I r_B(\alpha_I, \beta_I) = 0 \quad (30b)$$

$$\frac{1}{Pe_{II}} \frac{d^2 \alpha_{II}}{dz^2} - \frac{d\alpha_{II}}{dz} + \tau_{II} r_A(\alpha_{II}, \beta_{II}) = 0 \quad (30c)$$

$$\frac{1}{Pe_{II}} \frac{d^2 \beta_{II}}{dz^2} - \frac{d\beta_{II}}{dz} + \tau_{II} r_B(\alpha_{II}, \beta_{II}) = 0 \quad (30d)$$

where *Pe* is Peclet number defined as $Pe = \frac{u_1 H}{D_m}$. The mixing node equations are identical with Equations (21).

The formulation of adequate boundary conditions is required for solving the above system of equations. For zone *I*, they have the following form:

$$\frac{1}{Pe_I} \frac{d\alpha_I(0)}{dh} - \alpha_I(0) + \alpha_0 = 0 \quad (31a)$$

$$\frac{1}{Pe_I} \frac{d\beta_I(0)}{dh} - \beta_I(0) + \beta_0 = 0 \quad (31b)$$

$$\frac{d\alpha_I(1)}{dz} = 0 \quad (31c)$$

$$\frac{d\beta_I(1)}{dz} = 0 \quad (31d)$$

whereas for zone II:

$$\frac{1}{Pe_{II}} \frac{d\alpha_{II}(0)}{dh} - \alpha_{II}(0) + \alpha_I(1) = 0 \quad (32a)$$

$$\frac{1}{Pe_{II}} \frac{d\beta_{II}(0)}{dh} - \beta_{II}(0) + \beta_I(1) = 0 \quad (32b)$$

$$\frac{d\alpha_{II}(1)}{dz} = 0 \quad (32c)$$

$$\frac{d\beta_{II}(1)}{dz} = 0 \quad (32d)$$

5.6. Model No. 6 – dispersion flow in zones I and II, complete mixing in zone III, hydrodynamic regime A (ADM-A-D)

It is necessary to complete the model Equations (30) with Equations (22) describing carbonaceous substrate and biomass balances if degassing zone (III) is considered to occur. Additionally, boundary conditions for zone II will be redefined to the form:

$$\frac{1}{Pe_{II}} \frac{d\alpha_{II}(0)}{dh} - \alpha_{II}(0) + \alpha_{III} = 0 \quad (33a)$$

$$\frac{1}{Pe_{II}} \frac{d\beta_{II}(0)}{dh} - \beta_{II}(0) + \beta_{III} = 0 \quad (33b)$$

Volume distribution coefficients ζ_i and residence time τ_i in i -th zone defined as for model No. 2 indicated as PFM-A-D, i.e. Equations (24) and (25) should be included in the model equations.

5.7. Model No. 7 – dispersion flow in zones I and II, lack of zone III, hydrodynamic regime C (ADM-C)

The expression of residence time in zone II – τ_{II} including gas phase in this zone should be modified in order to formulate balance equations. This expression is compatible with Equation (27), similarly as for model No. 3 indicated as PFM-C.

5.8. Model No. 8 – dispersion flow in zones I and II, complete mixing in zone III, hydrodynamic regime C (ADM-C-D)

During the formation of model No. 8, model No. 5 were assumed as the basis. Then, it was completed identically as in models Nos. 6 and 7, i.e. the degassing zone's presence was included by completing

Equations (30) with Equations (22) describing carbonaceous substrate and biomass balances in this zone. Also residence time in zone *II* - τ_{II} including the gas phase was redefined. Such a procedure is identical with that performed in an analogical situation for the plug flow, i.e. in model No. 5.

Similarly as for plug flow models in zones *I* and *II*, the presence of identical core of balance equations for all the analysed cases can be observed during the formulation of axial dispersion models in these zones. This core is completed with further equations related to the introduction of zone *III* into the model. Regarding hydrodynamic regime *C* in the mathematical model results in introducing the modification of expressions which define the model parameters, i.e. mean residence times in zones and volume distribution coefficient.

There is some invariable core of balance equations in both analysed groups of mathematical models, that is in models characterised by the plug flow in zones *I* and *II* as well as in the axial dispersion models. This core of equations is being completed along with the increase of model complexity. The introduction of zone *III* results in adding the same expressions, i.e. equations characteristic for this zone. Mathematical description of the reactor operating in the hydrodynamic regime *C* requires only redefining parameters occurring in the model characterising the hydrodynamic regime *A*. This way of forming and modifying the equations demonstrates that models describing the airlift bioreactor under the assumed hydrodynamic conditions are similar in the mathematical structure.

6. SIMULATION CALCULATIONS AND QUANTITATIVE COMPARISON OF MODELS

The mathematical models shown above constitute the base for analysing airlift bioreactor operation under defined hydrodynamic conditions, i.e. in the hydrodynamic regime *A* or *C* and for the assumed structure of media flow, i.e. for plug flow or dispersion flow. The appropriate boundary value problems were solved in order to obtain distributions of the degree of conversion of the carbonaceous substrate and biomass dimensionless concentration as the functions of the reactor's length. Differential equations were integrated using the fourth order Runge-Kutta method. Newton algorithm was used to fit boundary conditions among the reactor zones. The computations were performed for selected process parameters. The obtained results are shown as graphs of $\alpha(z)$ function.

The calculations were performed for the bioreactor with a liquid internal loop and the following design dimensions: zone *I* height - $H_I = 1.75$ [m], zone *I* internal diameters - $d_I = 0.064, 0.054$ and 0.044 [m], zone *II* internal diameter - $d_{II} = 0.08$ [m]. These are the parameters of the reactor, for which the experimental verification of hydrodynamic model was described in earlier papers (Grzywacz, 2008 and 2009). The following values of process parameters were used in the computations: $\tau = 8, 10, 15$ [h], $c_{Af} = 0.08, 0.1, 0.12$ [kg/m³]. All the numerical simulations presented below were performed for the values of process parameters which correspond to stable steady states.

The degree of conversion profiles of carbonaceous substrate $\alpha(z)$ obtained within the numerical simulations were compared according to the following scheme:

- overall results of calculations for all the analysed models, at fixed, identical process conditions,
- determination of the impact of the assumed structure of the liquid phase stream,
- determination of the impact of selected process parameters,
- determination of the effect of the riser size,
- determination of the effect of the degassing zone size.

At first, the results of calculations according to particular models for fixed identical process conditions were compared. These comparisons were made for both, previously mentioned, hydrodynamic regimes, i.e. for the hydrodynamic regime *A* (Figure 3a) and the hydrodynamic regime *C* (Figure 3b). The graphs show that the obtained profiles have a similar qualitative course, and quantitative differences

between them are minor for all the analysed cases, i.e. for models Nos. 1, 2, 5, 6 for the hydrodynamic regime *A* and for models Nos. 3, 4, 7, 8 for the hydrodynamic regime *C*.

The next comparison regards the results of simulations for the plug flow bioreactor model and the axial dispersion model. Calculations for the dispersion flow were made for the following values of Peclet number $Pe_I = 2, 10, 20, 40$. Researchers agree that Peclet numbers are twice or three times as high as in zone *I*. Therefore, the values of Peclet numbers in zone *II* equal to $Pe_{II} = 4, 20, 40, 80$ were used for the simulation. The profiles of the degree of conversion determined for the dispersion flow and plug flow models are shown in Figure 4. It can be observed that the results of simulations for the same hydrodynamic regimes but with the dispersion flow are characterised by a higher conversion degree than those for the plug flow. However, the impact of Peclet number is minor.

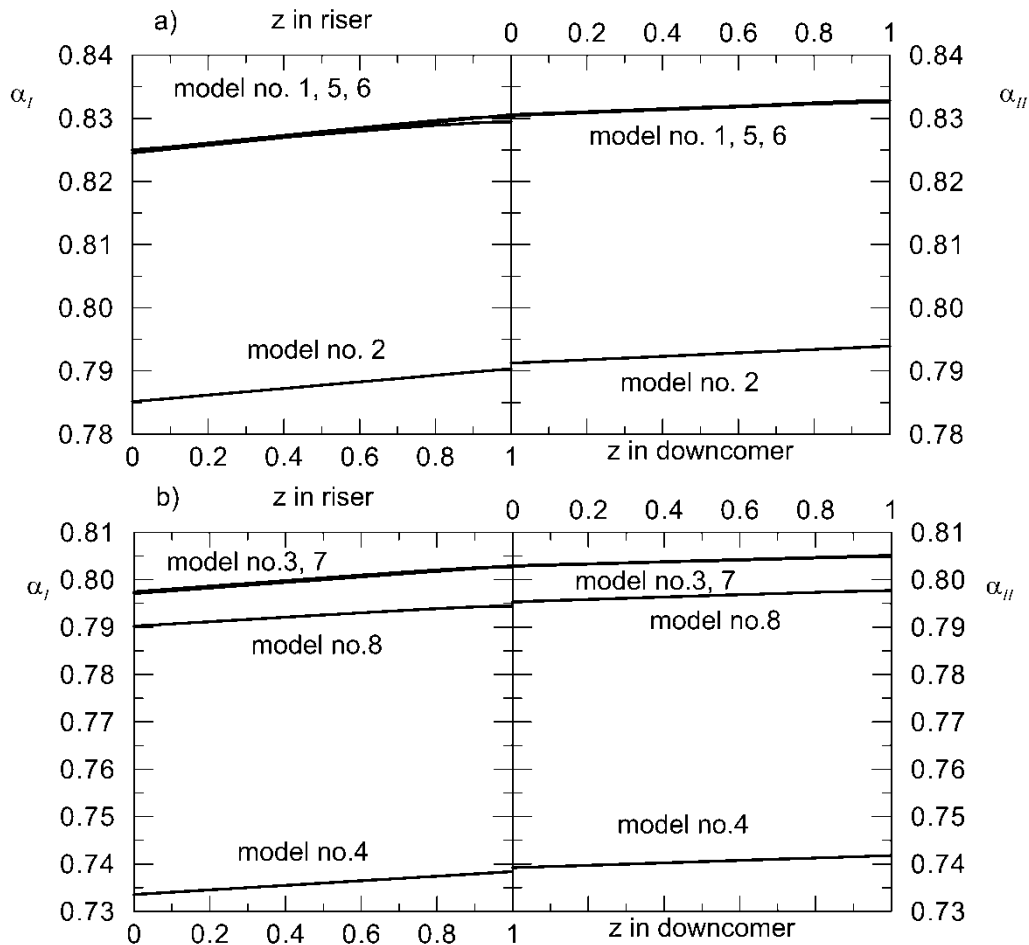


Fig. 3. Comparison of the degree of conversion of carbonaceous substrate $\alpha(z)$ obtained from models No. 1, 2, 5 and 6 for hydrodynamic regime *A*; a) ($\tau = 10$ [h], $c_{Af} = 0.1$ [kg/m³], $u_{0g} = 0.002$ [m/s], $d_I = 0.064$ [m], $Pe_I = 10$, $Pe_{II} = 20$) and results for models no. 3, 4, 7 and 8 describing hydrodynamic regime *C*; b) ($\tau = 10$ [h], $c_{Af} = 0.1$ [kg/m³], $u_{0g} = 0.035$ [m/s], $d_I = 0.064$ [m], $Pe_I = 10$, $Pe_{II} = 20$)

Then, the effects of fundamental operating parameters on the obtained degrees of conversion of the carbonaceous substrate were compared. Firstly, the computations were made for selected residence time values of liquid phase in the reactor (Figure 5). The presented results correspond to the expectations, i.e. the higher the residence time τ , the higher the carbonaceous substrate conversion degree. Further simulations were made for some selected values of carbonaceous substrate concentration at the inlet stream, i.e. for $c_{Af} = 0.05, 0.1, 0.2$ and 0.4 (Figure 6). As can be observed, increased c_{Af} demonstrates the inhibitory impact of the carbonaceous substrate. And then, an analysis of the effect of fed gas (air) quantity, and its superficial velocity u_{0g} , was performed. The results of these

calculations are presented in Figure 7. Gas hold-up increases along with u_{0g} (cf. Figure 2). Given that, the degree of conversion α is reduced. This can be explained in the following way. If oxygen is not the limiting substrate because of assuming sufficient aeration of reaction mixture, the supplied air affects only the bioreactor hydrodynamics. The presence of oxygen in zones of bioreactor, in which biodegradation occurs, reduces the liquid volume. Then, the reduction of the carbonaceous substrate conversion degree is observed.

The determination of reactor geometry impact on the obtained values of the carbonaceous substrate conversion degree was the next step of the analysis. In the research, changes in bioreactor geometry were simulated by changing the volume of the distribution coefficient ζ_I . According to the definition (21), this coefficient is the ratio of zone I volume to the whole volume of the reactor. Calculations were made for three values of coefficient ζ_I : 0.33, 0.51 and 0.77. The obtained conversion degrees of the carbonaceous substrate differed depending on the hydrodynamic regime, for which the calculations were made. For the hydrodynamic regime A, the obtained results of simulations were presented in Figure 8a, whereas for the hydrodynamic regime C in Figure 8b. For both cases, that is for the hydrodynamic regime A and the hydrodynamic regime C, the increase of ζ_I causes a reduction of the carbonaceous substrate conversion degree at the outlet from zone II. A higher value of ζ_I coefficient means a lower volume for zone II, and lower values for the degree of conversion $\alpha_{II}(1)$. A degree of conversion of the carbonaceous substrate at the outlet from zone I acts differently when coefficient ζ_I increases. For the reactor operation in the hydrodynamic regime A, an increased volume distribution coefficient ζ_I causes an increase of $\alpha_I(1)$, whereas for the reactor operation in the hydrodynamic regime C, an increase of volume distribution coefficient ζ_I causes a reduction of the conversion degree. It shall be emphasised that, according to Figure 1, the bioreactor ability to degrade the carbonaceous substrate depends on the carbonaceous substrate conversion degree at the outlet from zone I provided that the degassing zone is not present, or from zone III if the degassing zone is present. Therefore, this conversion degree should be maximised. Thus, if the bioreactor operates in the hydrodynamic regime A, then it is advantageous to increase the volume of zone I, only if sufficient aeration conditions are met. However, if biodegradation occurs in the hydrodynamic regime C, then the reactor should be designed so as zone I had a smaller volume than zone II.

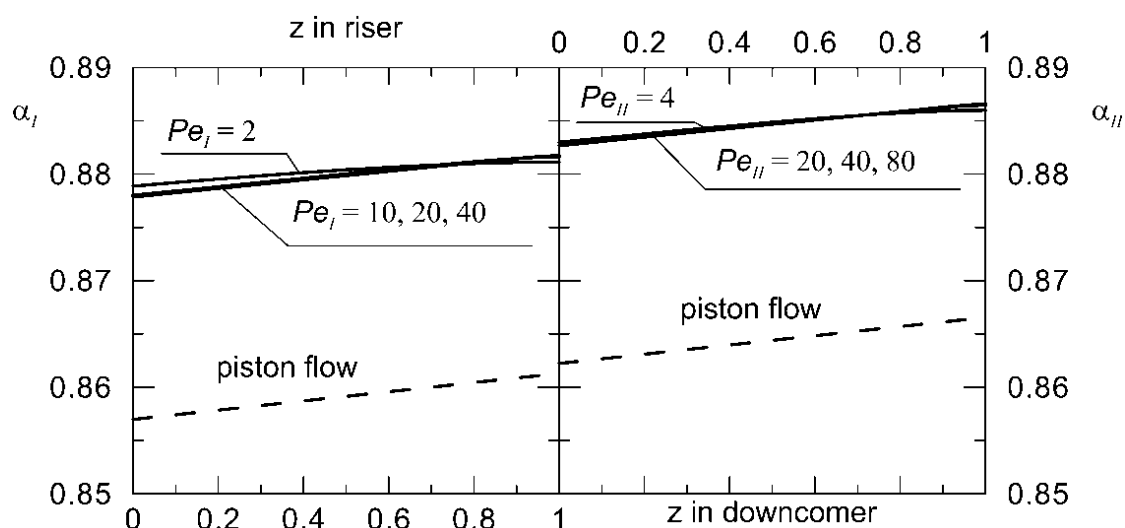


Fig. 4. Comparison of the simulation results for model with plug flow media (-----) with simulation results for model with dispersion flow media (—) for various Peclet number, for hydrodynamic regime C with degassing zone; $\tau = 15$ [h], $c_{Af} = 0.1$ [kg/m³], $u_{0g} = 0.07$ [m/s], $d_I = 0.064$ [m], $\zeta_{III} = 0.1$

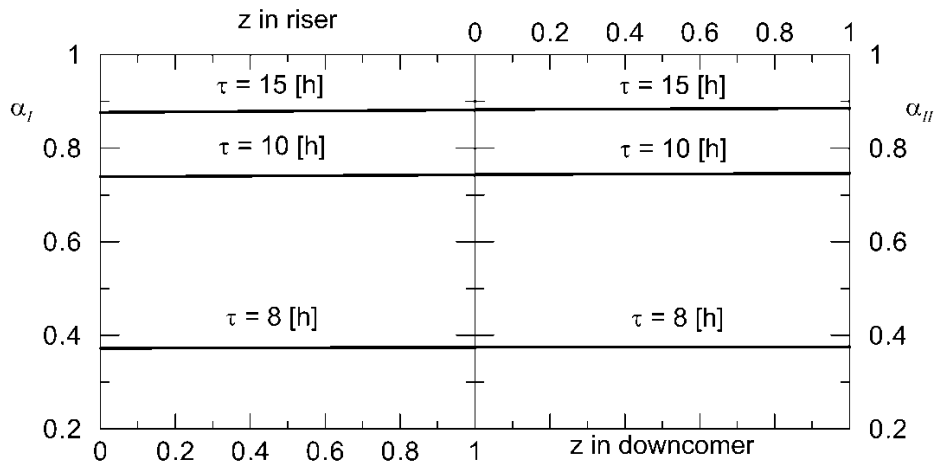


Fig. 5. Simulation results for various liquid residence time values in bioreactor. Calculations for model with dispersion flow and for hydrodynamic regime C with degassing zone; $c_{Af} = 0.1$ [kg/m³], $u_{0g} = 0.07$ [m/s], $d_I = 0.064$ [m], $\zeta_{III} = 0.1$, $Pe_I = 10$, $Pe_{II} = 20$

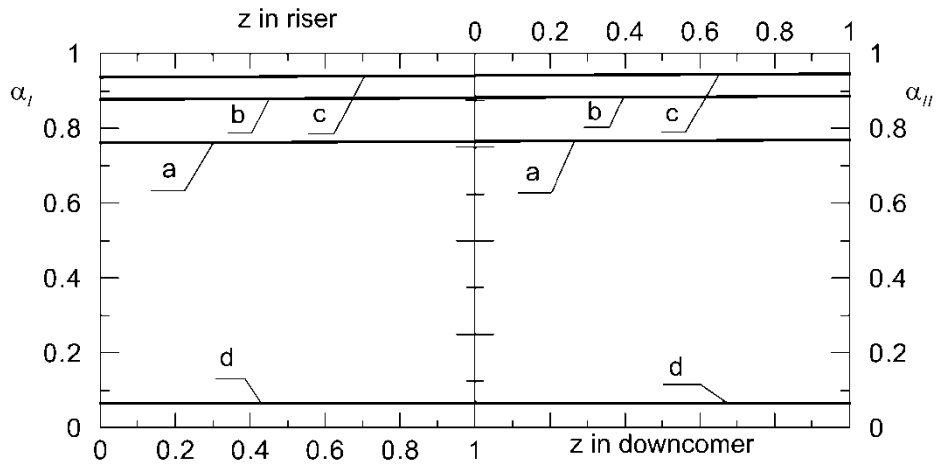


Fig. 6. Simulation results for chosen concentration of carbonaceous substrate at the inlet stream: a) 0.05, b) 0.1, c) 0.2 i d) 0.4. Calculations for model with dispersion flow and for hydrodynamic regime C with degassing zone; $c_{Af} = 0.1$ [kg/m³], $u_{0g} = 0.07$ [m/s], $d_I = 0.064$ [m], $\zeta_{III} = 0.1$, $Pe_I = 10$, $Pe_{II} = 20$

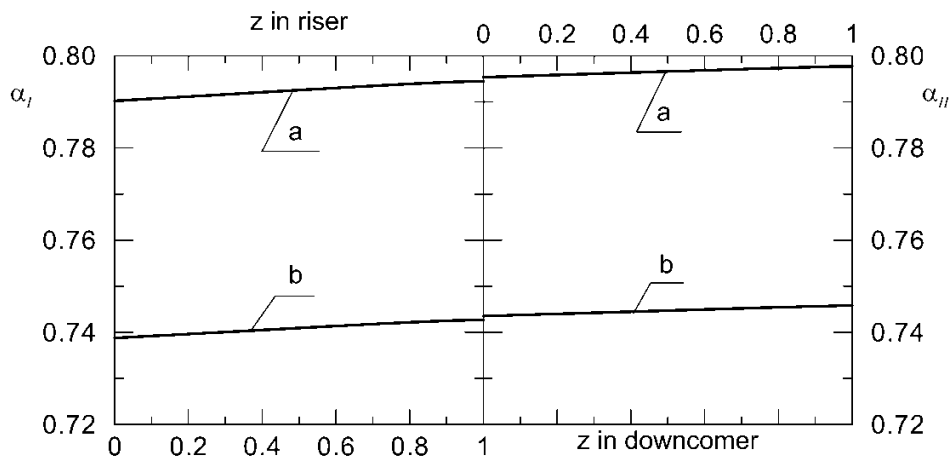


Fig. 7. Influence of superficial gas velocity (u_{0g}) on degree of conversion of carbonaceous substrate. Model with dispersion flow and for hydrodynamic regime C with degassing zone. a) $u_{0g} = 0.035$ [m/s] ($\epsilon_{gl} = 0.1$), b) $u_{0g} = 0.07$ [m/s] ($\epsilon_{gl} = 0.2$); $\tau = 10$ [h], $c_{Af} = 0.1$ [kg/m³], $d_I = 0.064$ [m], $\zeta_{III} = 0.1$, $Pe_I = 10$, $Pe_{II} = 20$

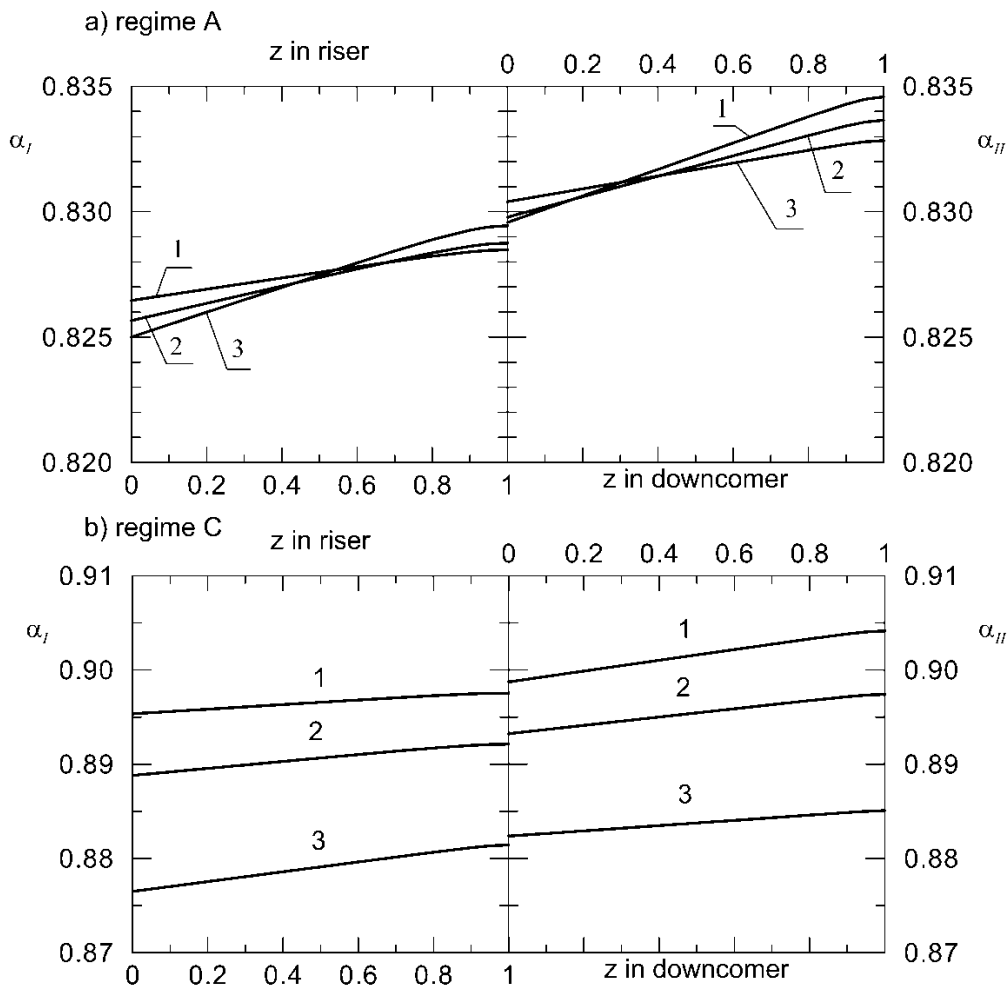


Fig. 8. Influence of riser volume (zone I) on degree of conversion of carbonaceous substrate: 1) $\zeta_I = 0.33$, 2) $\zeta_I = 0.51$, 3) $\zeta_I = 0.73$. a) Regime A – Calculations for model with dispersion flow and for hydrodynamic regime A with degassing zone. $\tau = 15$ [h], $c_{Af} = 0.1$ [kg/m³], $\zeta_{III} = 0.1$, $Pe_I = 10$, $Pe_{II} = 20$; b) Regime C – Calculations for model with dispersion flow and for hydrodynamic regime C with degassing zone. $\tau = 15$ [h], $c_{Af} = 0.1$ [kg/m³], $\zeta_{III} = 0.1$, $Pe_I = 10$, $Pe_{II} = 20$

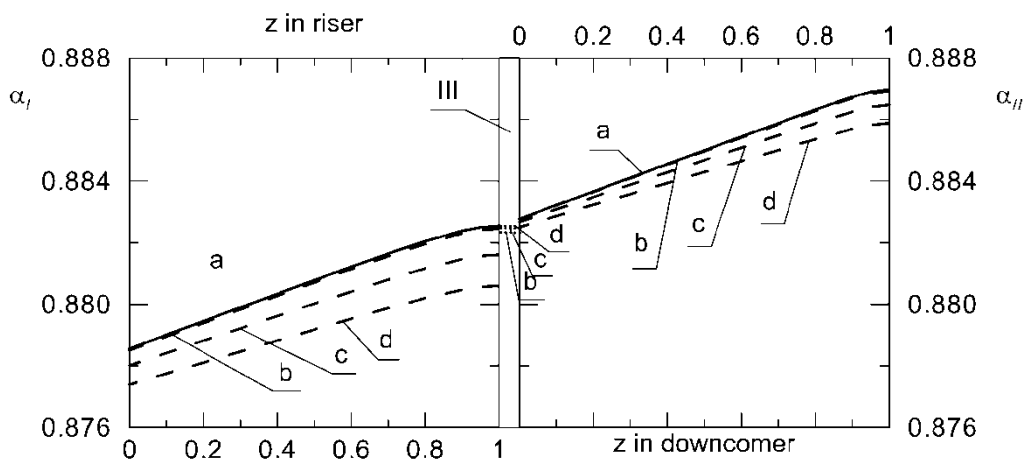


Fig. 9. Comparison of the simulation results for model without degassing zone (a - —) with the results for model with degassing zone (---) for various volume this zone: b) $\zeta_{III} = 0.01$, c) $\zeta_{III} = 0.1$, d) $\zeta_{III} = 0.2$; Dot lines (.....) signed the degree of conversion of the carbonaceous substrate at the inlet of zone III. Calculations for the model with the dispersion flow and for hydrodynamic regime C; $\tau = 15$ [h], $c_{Af} = 0.1$ [kg/m³], $d_i = 0.064$ [m], $Pe_I = 10$, $Pe_{II} = 20$

The other analysed parameter was volume of the degassing zone. Three volumes of the degassing zone *III* with three corresponding coefficients ζ_{III} presented below were analysed: 0.01, 0.1 and 0.2. The obtained results were compared with profiles for the case without the degassing zone. The comparison results are presented in Figure 9. It can be observed that the presence of zone *III* reduces the degree of the carbonaceous substrate conversion at the outlet from zones *I* and *II*. As has already been mentioned, for the presence of zone *III*, the bioreactor output depends on the value of conversion degree at the outlet from this zone. Therefore, the carbonaceous substrate conversion degree at the outlet from zone *III* is also marked in this figure. As can be observed, an increased volume of zone *III* at a constant volume of zone *I* has practically no impact on the reactor output. That is because an extra biodegradation of the carbonaceous substrate in zone *III* occurs, practically up to the values obtained with the models without the degassing zone. In that case, the assumption of such a small effect of the presence of the degassing zone on the carbonaceous substrate conversion degree at the outlet from the reactor is correct. So, it is possible to use the models without zone *III*. The presence of this zone has only the design significance related to the possible complete degassing of the reaction mixture, if the reactor is to operate in the hydrodynamic regime *A*.

7. CONCLUSIONS

This paper presents eight mathematical models of the airlift bioreactor, in which aerobic biodegradation of the carbonaceous substrate occurs. All the presented models belong to the family of single-substrate models which are derived from the assumption of sufficient aeration of all the zones in the analysed bioreactor. The presented models were formulated for two main hydrodynamic regimes for the reactor operation, i.e. the hydrodynamic regime *A* and the hydrodynamic regime *C*. Additionally, the presence of the degassing zone *III* or its lack was included in the formation of these models. Two structures of the liquid phase flow, namely the plug flow and the dispersion flow through the reactor zones *I* and *II* were assumed.

The algorithms of determining the carbonaceous substrate conversion profiles and biomass dimensionless concentration profiles as the function of the length of particular zones were prepared and coded for all the proposed models. A series of comparative computations for selected process and design parameters were made using the prepared software. The simulations were conducted to compare the effect of the hydrodynamic structures on the values of substrate conversion degrees.

The following conclusions can be drawn following the analysis of the obtained results.

- During the analysis of the effects of the assumed structure of the liquid phase streams in zones *I* and *II*, it can be noticed that the results of the simulation conducted for the same hydrodynamic regimes and for the assumed dispersion flow of media, always produces higher degrees of conversion of the carbonaceous substrate than those assuming the plug flow.
- An increase of the liquid mean residence time results in an increase of the carbonaceous substrate conversion degree. A similar result is observed for an increase in the concentration of the carbonaceous substrate in the feed stream. However, this refers only to relatively low values of c_{Af} . The inhibitory effect of the substrate is observed for high concentrations of the carbonaceous substrate in the feed stream. This results in a reduction of the carbonaceous substrate conversion degree.
- An interesting effect of zone *I* volume on the obtained degrees of the carbonaceous substrate conversions has been observed. If the bioreactor operates in the hydrodynamic regime *A*, then it is advantageous to increase the volume of zone *I*. Conversely, if biodegradation occurs in the hydrodynamic regime *C*, then the reactor should be designed so as zone *I* had a smaller volume than zone *II*.
- Also, the presence and size of the degassing zone in relation to the obtained degrees of the carbonaceous substrate conversion were analysed. An increase of zone *III* volume reduces the

obtained conversion degrees α at the outlet from reactor zones *I* and *II*. However, it does not significantly reduce of the bioreactor output. Regarding these observations, mathematical models with excluded the presence of zone *III* can be applied for the simulation and design of such bioreactors.

- The formulated mathematical models and the obtained results can be applied in design and analysis, or used for optimisation of carbonaceous substrate aerobic biodegradation processes with the assumption that all hydrodynamic zones of the airlift bioreactor are sufficiently aerated.

SYMBOLS

c_{Ai}	mass concentration of carbonaceous substrate in <i>i</i> -th zone, kg/m ³
c_{Bi}	mass concentration of biomass in <i>i</i> -th zone, kg/m ³
d_i	diameter of <i>i</i> -th zone, m
D_{mi}	coefficient of liquid dispersion in <i>i</i> -th zone, m ² /s
F_{Vi}	flow rate in <i>i</i> -th zone, m ³ /h
g	gravitational constant, m ² /s
h	current height, m
H_i	height of <i>i</i> -th zone, m
k, K_A, K_m	kinetic coefficients in Haldane equation
k_{fi}	coefficient of flow resistance in <i>i</i> -th zone
Pe_i	Peclet number in <i>i</i> -th zone
r_A, r_B	reaction rate with reference to reagent <i>A</i> and <i>B</i> , kg/(m ³ s)
u_{0l}, u_{0g}	superficial velocity of liquid and gas, respectively, m/s
u_{li}	velocity of liquid flow in <i>i</i> -th zone, m/s
V, V_i	total volume and volume of <i>i</i> -th zone, respectively, m ³
w_{BA}	yield coefficients of biomass in relation to substrate <i>A</i>
z	current coordinate of dimensionless length of reactor

Greek symbols

α_i	degree of conversion of carbonaceous substrate in <i>i</i> -th zone
β_i	dimensionless concentration of biomass in <i>i</i> -th zone
ε_{gi}	gas hold-up in <i>i</i> -th zone
ζ_i	volume distribution coefficient in <i>i</i> -th zone
ζ	recirculation ratio
ρ	density, kg/m ³
σ	surface tension, J/m ²
τ, τ_i	total and mean residence time of liquid in <i>i</i> -th zone, respectively, h
v	slip velocity of gas bubbles

Subscripts

<i>I, II, III, IV</i>	refer to the zone of a given number
<i>0</i>	refers to conditions behind the mixing point
<i>A</i>	refers to carbonaceous substrate
<i>A, B, C</i>	refer to hydrodynamic regime
<i>B</i>	refers to biomass
<i>f</i>	refers to conditions at the inlet to the reactor
<i>g</i>	refers to gas phase
<i>i</i>	<i>i</i> -th zone
<i>l</i>	refers to liquid phase

REFERENCES

- Báleš V., Antošová M., 1999. Mathematical and experimental modelling of phenol degradation in air-lift bioreactors. *Environ. Eng. Policy*, 1, 209-216. DOI: 10.1007/s100220050024.
- Boyadjiev Ch., 2006. On the modelling of an airlift reactor. *Int. Journal Heat Mass Transf.*, 49, 2053-2057. DOI: 10.1016/j.ijheatmasstransfer.2006.01.015.
- Camarasa E., Carvalho E., Meleiro L.A.C., Maciel Filho R., Domingues A., Wild G., Poncin S., Midoux N., Bouillard J., 2001. Development of a complete model for an air-lift reactor. *Chem. Eng. Sci.*, 56, 493-502. DOI: 10.1016/S0009-2509(00)00253-0.
- García Calvo E., Letón P., Arranz M.A., 1991. Prediction of gas holdup and liquid velocity in airlift loop reactors containing highly viscous Newtonian liquids. *Chem. Eng. Sci.*, 46, 2951-2954. DOI: 10.1016/0009-2509(91)85165-T.
- Gavrilescu M., Tudose R.Z., 1998 Concentric-tube airlift bioreactors. Part I: Effects of geometry on gas holdup. *Bioprocess Eng.*, 19, 37-44. DOI: 10.1007/s004490050480.
- Grzywacz R., 2008. Experimental verification of hydrodynamic models for airlift reactor. *Technical Journal – Mechanics. Cracow University of Technology*, (105) 5-M, 151-158.
- Grzywacz R., 2009. Influence of construction and process parameters on gas holdup coefficient in downcomer of airlift reactor. *Inż. Aparat. Chem.*, 48, 76-78.
- Grzywacz R., Lubaś P., 2006. Effect of operational conditions on the aeration of an airlift reactor. Analysis of the steady states. *Chem. Process Eng.*, 27, 1361-1376.
- Heijnen J.J., Hols J., van der Lans R.G.J.M., van Leeuwen H.L.J.M., Mulder A., Weltevrede R., 1997. A simple hydrodynamic model for the liquid circulation velocity in a full scale two- and three-phase internal airlift reactor operating in the gas recirculation regime. *Chem. Eng. Sci.*, 52, 2527-2540. DOI: 10.1016/S0009-2509(97)00070-5.
- Kanai T., Ichikawa J., Yoshikawa H., Kawase Y., 2000. Dynamic modelling and simulation of continuous airlift bioreactors. *Bioproc. Eng.*, 23, 213-220. DOI: 10.1007/s004499900154.
- Kanai T., Uzumaki T., Kawase Y., 1996. Simulation of airlift bioreactors: Steady-state performance of continuous culture processes. *Comp. Chem. Eng.*, 20, 1089-1099. DOI: 10.1016/0098-1354(95)00225-1.
- Korpajarvi J., Oinas P., Reunanen J., 1999. Hydrodynamics and mass transfer in an airlift reactor. *Chem. Eng. Sci.*, 54, 2255-2262. DOI: 10.1016/S0009-2509(98)00439-4.
- Marchuk J.C., Stein Y., Mateles R.I., 1980. Distributed parameter model of an airlift fermentor. *Biotechnol. Bioeng.*, 22, 1189-1211. DOI: 10.1002/bit.260220607.
- Pawlowsky U., Howell J.A., 1973. Mixed culture biooxidation of phenol. I. Determination of kinetic parameters. *Biotechnol. Bioeng.*, 15, 889-896. DOI: 10.1002/bit.260150506.
- Sikula I., Markoš J., 2008. Modelling of enzymatic reaction in an airlift reactor using an axial dispersion model. *Chemical Papers*, 62, 10-17. DOI: 10.2478/s11696-007-0073-9.
- Vial Ch., Poncin S., Wild G., Midoux N., 2001. A simple method for regime identification and flow characterisation in bubble columns and airlift reactors. *Chem. Eng. Proc.*, 40, 135-151. DOI: 10.1016/S0255-2701(00)00133-1.
- Znad H., Báleš V., Markoš J., Kawase Y., 2004. Modelling and simulation of airlift bioreactors. *Biochem. Eng. Journal.*, 21, 73-81. DOI: 10.1016/j.bej.2004.05.005.

Received 21 September 2011

Received in revised form 13 June 2012

Accepted 14 June 2012